

## Photoelectric Junctions Between GaAs and Photosynthetic Reaction Center Protein

Ludmila Frolov,<sup>†</sup> Yossi Rosenwaks,<sup>‡</sup> Shachar Richter,<sup>§</sup> Chanoch Carmeli,<sup>†</sup> and Itai Carmeli\*<sup>§</sup>

Departments of Biochemistry, Physical Electronics and Physical Chemistry and The Center for Nanosciences and Nanotechnology, Tel Aviv University, Tel Aviv 69978, Israel

Received: January 21, 2008; Revised Manuscript Received: April 14, 2008

The electronic coupling between the photoactive proteins and semiconductors can be used for fabrication of a hybrid biosolid-state electrooptical devices. The robust cyanobacterial nanosized protein-chlorophyll complex photosystem I (PS I) can generate a photovoltage of 1 V with a quantum efficiency of  $\sim 1$  and can be used as a phototransistor gate. A functional dry-oriented junction was fabricated by covalently binding genetically engineered cysteine mutants of PS I to a chemisorbed small connecting molecules on the GaAs surface. Kelvin probe force microscopy measurements showed an induced photovoltage of 0.3 and  $-0.47$  V in PS I-coated *p*- and *n*-type GaAs, respectively. The photovoltage resulted from an opposite direction of charge transfer between PS I and the semiconductors due to a difference of almost  $-0.8$  eV in the Fermi level energy of the *p*- and *n*-GaAs, thus providing direct evidence of an electronically coupled junction useable as a photosensor.

### Introduction

The electronic coupling between the photoactive proteins and semiconductors can be used for fabrication of a hybrid biosolid-state electro-optical devices. The robust cyanobacterial nanosized protein-chlorophyll complex photosystem I (PS I) can generate a photovoltage of 1 V with a quantum efficiency of  $\sim 1$  and can be used as a phototransistor gate. PS I is located in the thylakoid membranes of chloroplasts and cyanobacteria and mediates light-induced electron transfer.<sup>1</sup> The nanosized dimension, the generation of 1 V photovoltage, the absorbed energy conversion yield of approximately 47%, and a quantum efficiency of almost  $1^2$  makes the PS I reaction center a promising unit for applications in molecular nano-photoelectronics. The crystalline structure of PS I from *Synechococcus elongatus* and from the chloroplasts of plants has been resolved.<sup>3,4</sup> In cyanobacteria, the complex consists of 12 polypeptides, some of which bind 96 light-harvesting chlorophyll and 22 carotenoid pigment molecules. The electron transport chain in PS I contains a special pair of chlorophyll *a* (P700) that transfer electrons following photoexcitation in 1 ps (picosecond) to a monomeric chlorophyll *a* (Chl), through two intermediate phyloquinones (PQ) and three [4Fe-4S] iron sulfur centers (FeS), the final acceptors that are reduced in 0.2  $\mu$ s (Figure 1a). The cyanobacterial PS I is stable and can be used in fabrication of hybrid biosolid state devices. The structural stability of this is due to hydrophobic interactions that integrates 96 chlorophyll and 22 carotenoid pigment molecules and the trans membrane helixes of the core subunits.<sup>3</sup> The light-induced electron transfer at cryogenic temperatures<sup>5</sup> is an indication of little structural motions during function. In this work we demonstrate the formation of an electric junction between PS I and GaAs that generates a photovoltage of  $\sim 0.5$  V. PS I can enhance the photoelectronic properties of semi-

conductors when assembled as a photogate on a transistor, which can lead to the development of photosensors.

### Materials and Methods

**Sample Preparation.** The samples used in this study were undoped and *n* (Zn)- and *p* (Si)-doped GaAs (Wafer Technology LTD) with a doping concentration of  $1 \times 10^{18}$  cm<sup>-3</sup>. The properties of GaAs indicate Hall mobility of 54743, 65, and 2305 cm<sup>2</sup> V<sup>-1</sup> s<sup>-1</sup> and resistivity of 9<sup>8</sup>, 1<sup>-2</sup>, and 3<sup>-3</sup> for the undoped and *n*- and *p*-doped samples, respectively. The samples were cleaned for 10 min each in boiled acetone and then methanol, etched for 20 s in 5% HF, and finally rinsed for 8 s first in deionized water and then in ethanol. Organic molecules were attached through their carboxyl end to GaAs.<sup>6</sup> For chemical adsorption, the etched GaAs was immediately immersed for 8 h in an ethanol solution of 5 mM *N*- $\epsilon$ -maleimidocaproic acid (ECMA) or *N*- $\beta$ -maleimidopropionic acid (BMIPA) (Pierce Biotechnology Inc.) at 20 °C. The chemisorption was terminated by rinsing in aqueous solution. PS I molecules were indirectly attached to the surface by the formation of a covalent bond between the unique cysteine thiols in PS I mutants D235C/Y634C in PsaB subunits, and the maleimide moiety in the linker molecules was chemisorbed to the GaAs surface. The chemisorbed GaAs samples were rinsed in aqueous solution containing 20 mM Tris, pH 7, and 0.05%  $\beta$ -D-maltoside and immediately transferred to a solution containing the same buffer and 0.5 mg/ml chlorophyll of PS I for 2 h at 20 °C. After incubation, the sample was washed with deionized water and dried with ultrapure nitrogen.

**Site-directed Mutagenesis.** Site-directed mutagenesis was carried out in the *psaB* gene using the homologous recombination vector pZBL-D235C/Y634C. Mutations were inserted by an overlapping extension polymerase chain reaction (PCR). *psaB*-deficient recipient cells were transformed, and the transformants were grown under autotrophic growth conditions as previously described.<sup>7</sup>

**Preparation of PS I.** After the thylakoids were isolated from the cells, PS I was solubilized in the detergent *n*-dodecyl  $\beta$ -D-maltoside and successively purified on a DEAE-cellulose

\* Corresponding author. Phone: 972-3-6405714; Fax: 972-3-6405612; e-mail: itai@post.tau.ac.il.

<sup>†</sup> Department of Biochemistry.

<sup>‡</sup> Department of Physical Electronics.

<sup>§</sup> Department of Physical Chemistry and The Center for Nanosciences and Nanotechnology.

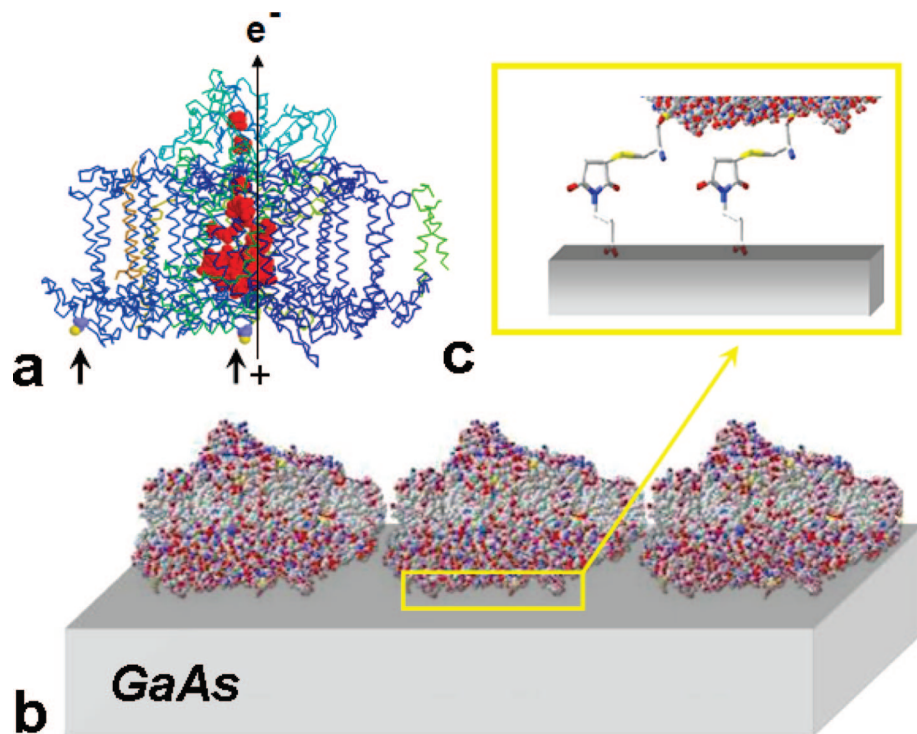


**Figure 1.** Molecular structure of PS I mutants and their monolayer coverage of GaAs. Light-induced charge separation (arrow) across the electron transport chain (space fill, red) in PS I modeled in a polypeptide back-boned structure with cysteine mutants D235C/Y634C shown in space fill, yellow (arrows) (a). A schematic presentation of a PS I monolayer (space fill model) on GaAs attached by the chemisorption of EMCA molecules (b). A zoom illustrate the binding of the EMCA molecule to the GaAs surface and the cysteine (rods) in PS I (c). Atom color codes are: C, gray; O, red; N, blue; and S, yellow. The images of the coordinates were modeled by Swiss PDB Viewer software in a PDB 1JB0 file.

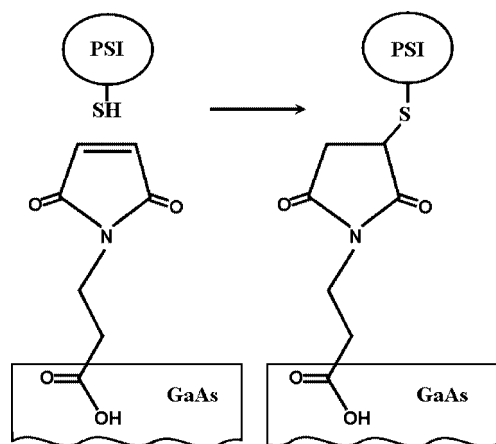


**Figure 2.** Covalent binding between PS I cysteine and maleimide in the linker molecules chemisorbed to GaAs. BMPA linker molecules are chemisorbed to the etched *n*- and *p*-type GaAs through their carboxyl end. The maleimide moiety readily reacted with the cysteine thiol and form covalent bond between the unique cysteines mutant of PS I and the linker molecule.

column and a sucrose gradient. The isolation of PS I, the analysis of subunit composition, and the protein and chlorophyll content were determined as described.<sup>7</sup> Surface-exposed cysteines on PS I were probed by biotin-maleimide, which specifically reacts with the sulfhydryl groups. Biotin-labeled PS I complexes were dissociated and separated by sodium dodecyl sulfate polyacrylamide gel electrophoresis. For immunoblot detection, protein samples were transferred from the gel to nitrocellulose, reacted with peroxidase-conjugated avidin, and then developed with enhanced chemiluminescence reagents as previously described. Measurements of P700 photooxidation at 700 nm and at 820 nm in thylakoids and PS I were carried out using a modified

flash photolysis setup as described in ref 8. The samples contained 50 mM Tris, pH 8, 10 mM sodium ascorbate, 0.5 mM dichlorophenol indophenol, and 25  $\mu\text{g}$  of chlorophyll per mL PS I complexes. Absorption change transients were analyzed by fitting with a multiexponential decay using Marquardt least-squares algorithm programs (KaleidaGraph 3.5 from Synergy Software, Reading, PA). The half-time for the decay of oxidized P700 was 25 ms in both the native and the D235C/Y634C mutant PS I.

**AFM and KPFM Measurements.** The atomic force microscopy (AFM) and Kelvin probe force microscopy (KPFM) measurements were conducted using both Nanoscope IIIa MultiMode with Extender Electronics Module, (Veeco Inc.), and Solver PH47, (NTMDT Inc.), operating in tapping mode at the cantilever resonance frequency of around 300 kHz. The electrostatic force was measured in the so-called “lift mode;” in this method, after the topography is measured, the tip is retracted from the sample surface to a fixed height. The oscillation of the tip is induced only by an external AC bias applied to the cantilever at the same resonance frequency previously used for the topography measurements in the tapping mode. The contact potential difference (CPD) is extracted in the conventional way by nullifying the output signal of a lock-in amplifier that measures the electrostatic force at the first resonance frequency.<sup>9</sup> The NTMDT AFM was equipped with a custom-made 1300 nm wavelength feedback laser to prevent any sample-induced photovoltage. Most CPD measurements were conducted in a nitrogen glovebox. A comparison with an in situ peeled pyrolytic graphite standard (OPG) enabled us to extract the actual work function of all measured samples. A He–Ne laser ( $\lambda = 632.8 \text{ nm}$ ,  $5 \text{ mW/cm}^2$ ) was used for the photovoltage measurements.

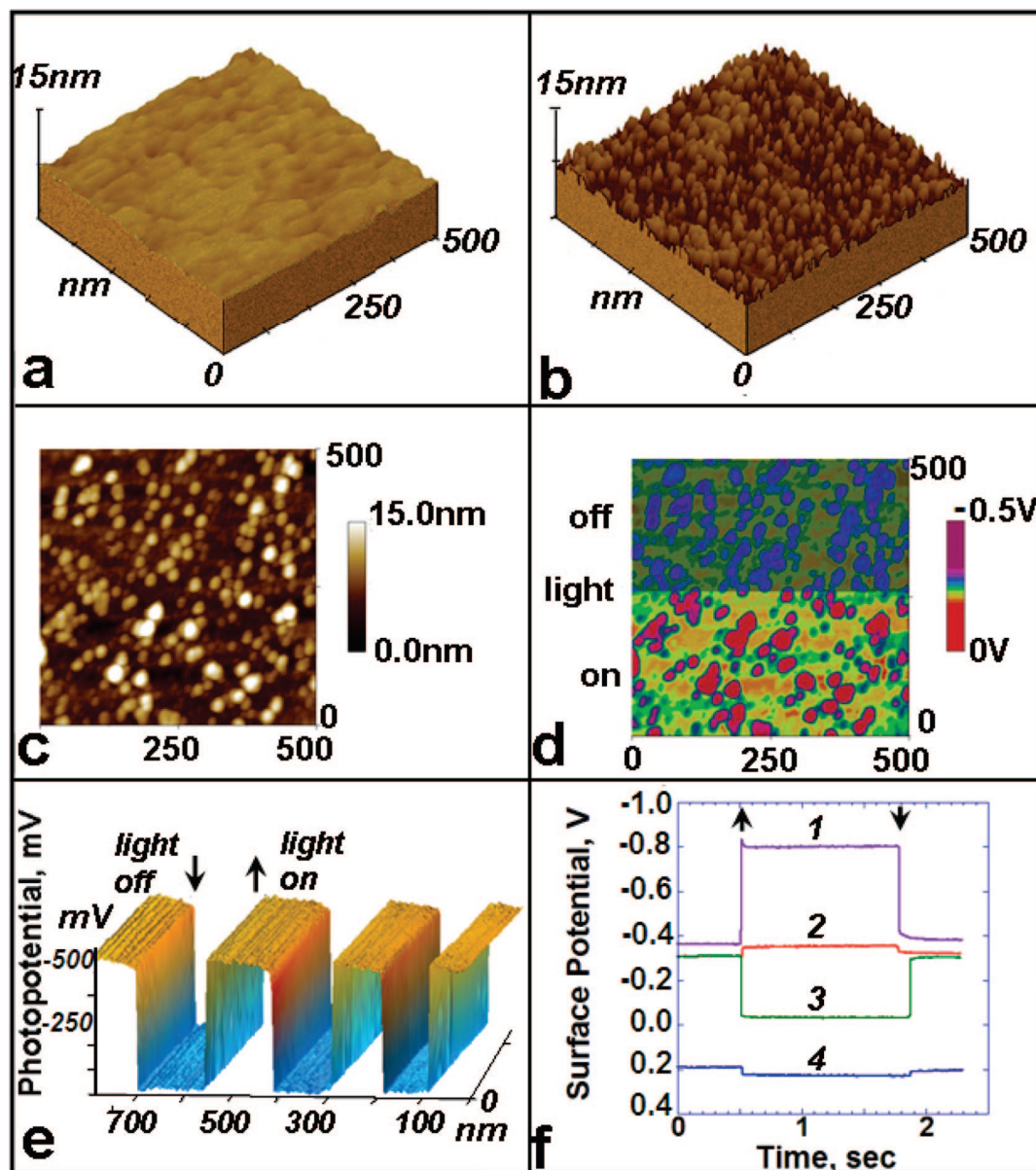


**Figure 3.** Two- and three-dimensional scanning probe microscopy images of the oriented PS I GaAs surface. Topographic 3D images of bare (a) and PS I monolayer covered (b) surfaces of GaAs; 2D topographic (c) and surface potential (d) images of the same set of PS I monolayer on GaAs surface. A light-induced PS I negative surface potential of PS I is seen in panel d. The illumination induced a fast reversible photovoltage image of a dense PS I monolayer on *n*-GaAs (e); the scanning directions for each raster of the constructed images were from top to bottom. (f) Kinetic traces of light-induced surface potential changes in GaAs with PS I [*n*-type (1), *p*-type (3)] and without fabricated monolayer [*n*-type (2) and *p*-type (4)]. Topography and surface potential measurements were done in AFM and KPFM modes, respectively. Illumination was provided by a He–Ne laser at 632.8 nm, 5 mW/cm<sup>2</sup>.

## Results and Discussion

To fabricate the oriented monolayer, genetically engineered unique mutations in PS I were used. The mutations were induced in the robust PS I reaction centers from the cyanobacterium *Synechocystis* sp. PCC 6803, in which all chlorophyll and carotenoids molecules are integrated into the core subunits complex. Mutations D235C/Y634C (Figure 1a) were selected near the P700 to secure close proximity on binding of the reaction center to the solid surface through the cysteines. This approach can facilitated efficient electronic junctions and avoided disturbance in the function of the reaction center. Mutations D235C/Y634C were induced by homologous recombination of *Synechocystis* sp. PCC 6803 recipient cell using the vectors and the methodology described earlier.<sup>7</sup> When the mutant cells were grown under autotrophic conditions, the

photochemical and structural properties of the isolated PS I did not change<sup>8</sup> (see Methods section).

The free thiols of PS I could not be bound directly to the GaAs surface because the chemisorption of molecules with free thiols and carboxyls requires the use of organic solvents. Therefore, we fabricated a self-assembled monolayer of *N*- $\epsilon$ -maleimidocaproic acid (EMCA) and *N*- $\beta$ -maleimidopropionic acid (BMPA) linker molecules (Figures 1b and 2) chemisorbed to the etched *n*- and *p*-type GaAs through their carboxyl end. The maleimide moiety readily reacted with the mutated cysteines D235C/Y634C to form a dense monolayer of PS I under aqueous conditions (Figure 2). The monolayer consists of particles having a diameter of about 15 and 20 nm (Figure 3b), corresponding to the size of monomers and trimers of PS I, respectively.<sup>3</sup> To determine the orientation, we have fabricated

TABLE 1: Contact Potential Difference of PS I Monolayer on GaAs

sample	Contact potential difference (V) <sup>a</sup>					
	<i>n</i> -GaAs		<i>p</i> -GaAs		<i>i</i> -GaAs	
	dark	photovoltage	dark	photovoltage	dark	photovoltage
GaAs	$-0.405 \pm 1 \times 10^{-3}$	-0.085	$0.350 \pm 1 \times 10^{-4}$	0.0420	$-0.023 \pm 3 \times 10^{-3}$	0.062
GaAs-EMCA	$-0.305 \pm 1 \times 10^{-4}$	-0.053	$0.520 \pm 5 \times 10^{-3}$	0.040	$0.160 \pm 5 \times 10^{-4}$	0.038
GaAs-EMCA-PSI	$-0.359 \pm 3 \times 10^{-4}$	-0.472	$-0.152 \pm 7 \times 10^{-4}$	0.295	$-0.144 \pm 1 \times 10^{-3}$	0.265
GaAs-BMPA-PSI	$-0.315 \pm 4 \times 10^{-4}$	-0.451	$-0.170 \pm 3 \times 10^{-3}$	0.248	$-0.185 \pm 8 \times 10^{-4}$	0.254

<sup>a</sup> The CPD of PS I reaction center monomers and trimers from a mutant D235C/Y634C monolayer on *n*-type, *p*-type, and undoped (*i*-) GaAs surfaces measured by KPFM.<sup>9</sup> Each value is an average of 6 samples of  $512 \times 512$  line scans of untreated, etched, and chemisorbed with EMCA and BMPA monolayers and a PS I monolayer attached to the base monolayer on GaAs measured in the dark or in the light. Illumination was provided by a He-Ne laser at 632.8 nm, 5 mW/cm<sup>2</sup>. All the CPD measurements were calibrated against highly oriented, freshly cleaved pyrolytic graphite that gave a CPD of 0.4 V.

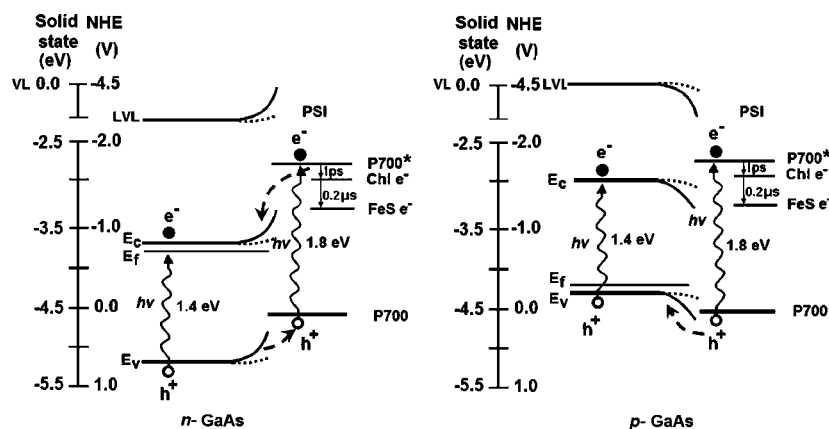


**Figure 4.** Schematic presentation of energy levels in a PS I in junction with *n*- and *p*-type GaAs. The *n*- and *p*-type GaAs band energies were determined by measurements of CPD compared to a graphite standard and from the published band gap energy.<sup>15</sup> The redox levels of electron carriers in PS I were assigned according to the potential measured against a normal hydrogen electrode (NHE).<sup>2</sup> The redox potentials measured at pH 7 were converted to NHE by addition of 0.414 V, which accounts to the difference in redox potential between pH 7 and NHE. The scale on the left shows the solid state energy levels in relation to the NHE redox levels.<sup>16</sup> The decrease in SPV is due to both electron transfer from the PS I monolayer to and a hole from *n*-type GaAs. The light-induced flattening of band bending is indicated (—). In the case of *p*-type GaAs, the increase in SPV results from a light-induced reduction of the FeS. The solid state energy levels were  $-3.8$ ,  $-3.7$ , and  $-5.2$  eV for the *n*-type and  $-4.43$ ,  $-3.15$ , and  $-4.53$  eV for the *p*-type GaAs Fermi-level ( $E_f$ ) and conduction- ( $E_c$ ) and valence-bands ( $E_v$ ), respectively. The energy levels in PS I were  $-4.58$ ,  $-3.06$ ,  $-3.52$  eV for the primary electron donor (P700), the primary (Chl), and the final (FeS) electron acceptors, respectively. Vacuum (VL) and local vacuum levels (LVL) are indicated.

a less dense monolayer in which the PS I molecules were spaced apart from each other on *p*-type GaAs. The topography of the monolayer was determined by atomic force microscopy (AFM) and the photovoltage by a novel Kelvin probe force microscopy system that uses a 1300 nm wavelength feedback laser. The topography was determined by scanning of the surfaces by the AFM cantilever tip in tapping mode. For surface potential measurements the surface was scanned by the KPFM conductive tip, which was placed  $\sim 20$  nm above the surface, and its deflection due to positive or negative surface potential was determined by the feedback circuit. The photovoltage of single PS I monomer and trimer complexes within the monolayer demonstrated a clear, light-induced potential in all PS I particles. The photovoltage was developed only where peaks ascribed to the PS I complexes were observed in the topographic image (Figure 3c–d). These findings clearly indicate that all the PS I complexes bound to the GaAs surface are functionally active and oriented in the same direction.

The etching and chemisorption of the EMCA and BMPA monolayers on the GaAs surface caused an increase of between 0.1 and 0.17 V in the contact potential difference (CPD) of the various GaAs surfaces (Table 1); this is probably due to the formation of Ga carboxylate and to the dipole formed by the two exposed oxygen atoms at the maleimide ring. Similar changes in the surface energetic of semiconductors are affected by the chemisorption of organic<sup>6</sup> and inorganic molecules<sup>10</sup> and

peptides used to modulate photonic crystals band gap energies.<sup>11</sup> The binding of PS I to the GaAs (Figure 1c) caused a sizable decrease in the CPD (without illumination) of 0.05, 0.31, and 0.67 V for the *n*-, *i*-, and *p*-doped GaAs-PS I, respectively (Table 1). The difference in CPD between the *n*- and *p*-type GaAs can be explained by electron transfer from the PS I to the *p*-GaAs with the help of the energy levels diagram shown in Figure 4, illustrating that the P700 ground-state energy level<sup>5</sup> is higher than the valence band maximum ( $E_v$ ) of both *p*- and *n*-GaAs. An electron, however, will be transferred from the P700 level to the *p*-GaAs valence band but not to the *n*-GaAs because the latter valence band is fully occupied. Such an oxidation of PS I will charge it positively and will decrease the CPD, in agreement with our measurements. Similar results were measured upon the binding of PS I to GaAs chemisorbed with a monolayer of BMPA, a similar molecular structure shorter by only one carbon atom than the EMCA. These results provided the first indication for a direct electron transfer between large proteins, through the chemisorbed small molecule, and the GaAs substrate.

A very small photovoltage of  $-0.05$ ,  $0.06$ , and  $0.04$  V was measured in the EMCA-treated *n*-, *i*-, and *p*-GaAs, respectively. The chemisorption of the PS I monolayer, however, resulted in a much higher photovoltage of about 0.265 and 0.295 V for the *i*- and *p*-doped GaAs, respectively (Table 1). Such a positive photovoltage is due to the light-induced charge separation and

consequent electron transfer across the protein, resulting in a dipole whose negative charge is at the reducing end of the PS I (away from the GaAs surface). These results are in agreement with earlier findings of light-induced generation of surface potential in dry single plant PS I molecules placed on mercaptoethanol-covered gold surface<sup>12</sup> and in dry oriented monolayers of cyanobacterial PS I on gold surface.<sup>7</sup> The dry PS I GaAs junction functioned for a tested duration of 1 y. Dry proteins which are stable for a year are expected to function much longer because of the slow down in chemical reactions that take place in solution.

Surprisingly, the PS I monolayer bound to *n*-GaAs induced a negative photovoltage of  $-0.47$  V; this opposite polarity could be due either to a change in the orientation of the PS I on binding or to a charge transfer to the GaAs. A change in the orientation of PS I is unlikely because the binding is caused by a covalent bond formation between the maleimide in the linker molecule and the unique cysteines in PS I, which are at the same location in the PS I used and therefore in all types of GaAs surfaces. Hence, the change in the photovoltage polarity can be explained by comparing the energy of the GaAs bands with the redox potential energy levels of the primary donor and the electron acceptors in the PS I protein, illustrated together in Figure 4. It should be emphasized that the KPFM tip is not in contact with the PS I (as in a solar cell for example), therefore its Fermi level does not coincide with the P700 and the FeS energy levels for *n*- and *p*-GaAs, respectively. The figure shows a difference of almost  $-0.8$  and  $-0.235$  eV in the energies of the Fermi level ( $E_f$ ) and in the conduction band minimum ( $E_c$ ) of *p*- and *n*-GaAs, respectively. The  $E_c$  of *n*-type GaAs is negative by about  $-0.5$  and  $-0.24$  eV relative to the primary (Chl) and the final electron acceptors (FeS) in PS I, respectively. Therefore, upon illumination, electrons will transfer from the PS I to the *n*-type GaAs, and the holes move to the PS I from the semiconductor valence band; this positively charges the PS I and decreases the surface potential (Figure 4). The charge transfer from the electronic excited-state of dye molecules adsorbed on TiO<sub>2</sub> at aqueous interfaces<sup>13</sup> resembles the function of the PS I protein–GaAs junction. Unlike charge exchange between PS I and GaAs reported here, the modulation of surface potential obtained by chemisorption of inorganic, organic, and small peptides<sup>10,11,14</sup> was mostly due to dipole interactions between the molecules and semiconductors.

Measurements of the dynamics of the formation and the decay of the steady state photovoltage revealed a reversible, light-induced change in the GaAs–PS I monolayer. The photovoltage onset was faster than the shutter on-and-off time of 0.7 ms (Figure 3f, graph lines 1 and 3). The rate of the major component (96%) of the total decay of the steady-state photovoltage had a fast unresolved  $t_{1/2}$ , due to a charge recombination in the PS I attached to the GaAs. Only about 4% of the CPD decay was due to charge recombination in GaAs, with a  $t_{1/2}$  value of 1.5 s (Figure 3f, graph lines 2 and 4) (Figure 5 and 6, Supporting Information). Remarkably, the observation that the decay rate of the light-induced steady state CPD in the dry PS I is faster than 0.7 ms, that is, in the range of the charge recombination rate between P700<sup>+</sup> and the reduced acceptors prior to the iron–sulfur cluster (the final acceptor, FeS) in PS I in aqueous solution,<sup>2</sup> supports our assumption that the PS I did not significantly change its function when chemisorbed to GaAs in a dry environment.

## Conclusion

We have proposed an approach in the use of a biological molecule in the modification and the interaction with inorganic semiconductors. An active electronic junction between the proteins and GaAs was fabricated by the self-assembly of a monolayer of oriented PS I. Unlike small molecules commonly used to modify solid state interfaces, the interaction of the PS I protein with GaAs involves charge transfer that causes a large decrease in the surface potential of *p*-GaAs but does not modify the negatively charged *n*-GaAs surface in the dark. Although the PS I monolayer has the same orientation on all crystals, it induced very large negative and positive photovoltage in both *n*-GaAs and *p*-GaAs, respectively, due to electron and hole transfer between the protein and GaAs. Such systems can be used to develop photogating of transistors that can be used as photosensors. This suggestion is supported by the recent demonstration of a use of PS I as a photogate on a FET transistor that was published<sup>17</sup> during the preparation of this manuscript. PS I was connected by a tatter extended from the quinone to a gold nanoparticle bound to a silan–thiol-modified Si. Unlike the PS I–GaAs tightly coupled junction, the wired PS I functioned only in solution and requires a counter electrode.

**Acknowledgment.** Thanks are due to the Institute of Nanoscience and Nanotechnology of Tel Aviv University for use of facilities.

**Supporting Information Available:** Figures mentioned within the text are provided. This material is available free of charge via the Internet at <http://pubs.acs.org>.

## References and Notes

- (1) Chitnis P. R.; Nelson, N. *Photosynthetic Apparatus: Molecular Biology and Operation*; Academic Press: New York, 1991; Chapter 5, pp 177–224.
- (2) Brettel, K.; Leibl, W. *Biochim. Biophys. Acta* **2001**, *1507*, 100–114.
- (3) Jordan, P.; Fromme, P.; Witt, H. T.; Klukas, O.; Saenger, W.; Krauss, N. *Nature* **2001**, *411*, 909–917.
- (4) Amunts, A.; Drory, O.; Nelson, N. *Nature* **2007**, *447*, 58–63.
- (5) Brettel, K. *Biochim. Biophys. Acta* **1997**, *1318*, 322–373.
- (6) Bastide, S.; Butruille, R.; Cahen, D.; Dutta, A.; Libman, J.; Shanzer, A.; Sun, L. M.; Vilan, A. *J. Phys. Chem. B* **1997**, *101*, 2678–2684.
- (7) Frolov, L.; Rosenwaks, Y.; Carmeli, C.; Carmeli, I. *Adv. Mater.* **2005**, *17*, 2434–2437.
- (8) Gong, X. M.; Agalarov, R.; Brettel, K.; Carmeli, C. *J. Biol. Chem.* **2003**, *278*, 19141–19150.
- (9) Shikler, R.; Fried, N.; Meoded, T.; Rosenwaks, Y. *Phys. Rev. B* **2000**, *61*, 11041–11046.
- (10) Liu, Y.; Komrowski, A. J.; Kummel, A. C. *Phys. Rev. Lett.* **1998**, *81*, 413–416.
- (11) Strauf, S.; Rakher, M. T.; Carmeli, I.; Hennessy, K.; Meier, C.; Badolato, A.; Dedood, M. J. A.; Petroff, P. M.; Hu, E. L.; Gwinn, E. G.; Bouwmeester, D. *Appl. Phys. Lett.* **2006**, *88*.
- (12) Lee, I.; Stubna, A.; Greenbaum, E. *J. Phys. Chem. B* **2000**, *104*, 2439–2443.
- (13) Wang, Q.; Carnpbell, W. M.; Bonfantani, E. E.; Jolley, K. W.; Officer, D. L.; Walsh, P. J.; Gordon, K.; Humphry-Baker, R.; Nazeeruddin, M. K.; Gratzel, M. *J. Phys. Chem. B* **2005**, *109*, 15397–15409.
- (14) Vilan, A.; Shanzer, A.; Cahen, D. *Nature* **2000**, *404*, 166–168.
- (15) Miller, R. J. D.; McLendon, G. L.; Nozik, A. J.; Schmickler, W.; Willig, F. *Surface Electron Transfer Processes*; VCH Publishers Inc.: New York, 1995.
- (16) Nozik, A. J. *Annu. Rev. Phys. Chem.* **1978**, *29*, 189–222.
- (17) Terasaki, N.; Yamamoto, N.; Tamada, K.; Hattori, M.; Hiraga, T.; Tohri, A.; Sato, I.; Iwai, M.; Taguchi, S. *Biochim. Biophys. Acta* **2007**, *1767*, 653–659.